Cell type specific analysis of ALS associated proteins reveals immune-regulated targets

Riham Ayoubi[1,2], Emma J. MacDougall[1,2], Ian McDowell[1,2], Marie-France Dorion[3,7], Jay P. Ross[4], Sara González Bolívar[1,2], Vera Ruiz Moleón[1,2], Charles Alende[1,2], Maryam Fotouhi[1,2], Mathilde Chaineau[3], Carol X.-Q. Chen[3], Valerio E.C. Piscopo[3], Vincent Soubannier[3], Gilles Maussion[3], Cecilia Rocha[3], Tracy Keates[5], Brian D. Marsden[5], Leonidas Koukouflis[5], Wen Hwa Lee[5], Edvard Wigren[6], Carolyn A. Marks[6], Luke M. Healy[7], Patrick A. Dion[2], Guy A. Rouleau[1,2], Edward A. Fon[1,2], Susanne Gräslund[6], Opher Gileadi[5,6], Aled M. Edwards[1,2], Thomas M. Durcan[3], Peter S. McPherson[1,2], Carl Laflamme[1,2]

Author affiliations:

[1]Structural Genomics Consortium, Montreal Neurological Institute-Hospital (The Neuro), McGill University, Montreal, H3A 2B4, Canada.

[2]Neurodegenenerative Diseases Research Group, Department of Neurology and Neurosurgery, Montreal Neurological Institute-Hospital (The Neuro), McGill University, Montreal, H3A 2B4, Canada.

[3]Early Drug Discovery Unit (EDDU), Department of Neurology and Neurosurgery, Montreal Neurological Institute-Hospital (The Neuro), McGill University, Montreal, H3A 2B4, Canada.

[4]Department of Genetics, Stanford University School of Medicine, Stanford, CA, 94305, USA

[5]Structural Genomics Consortium, University of Oxford, Oxford, OX3 7FZ, UK.

[6]Structural Genomics Consortium, Department of Medicine, Karolinska Institute, Solna, 171 76, Sweden

[7]Neuroimmunology Unit, Department of Neurology and Neurosurgery, Montreal Neurological Institute-Hospital (The Neuro), McGill University, Montreal, H3A 2B4, Canada.

Correspondence to: Carl Laflamme

Full address: McGill University, Montreal Neurological Institute, Room BT-205, 3801

University St., Montreal, QC, H3A 2B4, CANADA

E-mail: carl.laflamme@mcgill.ca

Running title: Immune-Regulated ALS Protein Targets

Keywords: oligodendrocyte; macrophage; astrocytes; interferon-gamma; lipopolysaccharide; RNA sequencing

Abstract

Amyotrophic lateral sclerosis (ALS) is a progressive neurodegenerative disorder characterized by the degeneration of upper and lower motor neurons. While four core familial ALS genes—*SOD1*, *C9orf72*, *FUS*, and *TARDBP*—have been extensively studied, more than 30 additional genes have recently been implicated in the disease, many of which remain poorly explored in ALS pathobiology. Using knock-out cells as controls, we characterized antibodies against 33 ALS-associated proteins, including ACSL5, ALS2, ANG, ANXA11, ATXN2, C9orf72, CAV1, CCNF, CHCHD10, CHMP2B, FIG4, FUS, HNRNPA1, HNRNPA2B1, KIF5A, LGALS1, MATR3, NEK1, OPTN, PFN1, SETX, SIGMAR1, SOD1, SPG11, SQSTM1, TAF15, TARDBP, TBK1, TIA1, TUBA4A, UBQLN2, VAPB, VCP, and profiled protein expression for these ALS proteins across human induced pluripotent stem cell (iPSC)-derived and primary neurological cell types (neurons and glia). We uncovered diverse and cell-type-specific expression signatures that were often not concordant with mRNA expression datasets. Notably, 22 proteins were expressed in glial populations, with ten dynamically regulated by inflammatory cues in microglia cells, underscoring immune-responsive pathways as important contributors to ALS pathogenesis.

Introduction

Amyotrophic lateral sclerosis (ALS) is an adult-onset neurodegenerative disorder characterized by the progressive loss of upper and lower motor neurons. ALS is polygenic in nature; the first ALS-associated gene, *SOD1*, was discovered in 1993,[1] and over 30 genes have been identified as linked to the familial or sporadic form of the disease.[2,3] Several cellular pathways have been implicated in ALS pathogenesis, including RNA metabolism, autophagy, lysosome function and other forms of protein homeostasis. Research has disproportionately focused on four well-characterized genes—*SOD1, C9orf72, FUS, and TARDBP*— while the majority of ALS-associated genes and their corresponding proteins remain largely unstudied.

The role of the immune system in ALS is increasingly recognized,[4] and mapping the expression of ALS-associated proteins in neuronal and glial cells is essential to guide therapeutic strategies. Although the prevailing assumption has been that ALS genes are primarily expressed in motor neurons, a recent preprint reported RNA-based clustering of ALS-associated genes into glial-enriched modules.[5] While RNA abundance provides a useful proxy for protein expression, mRNA and protein levels do not necessarily correlate due to post-transcriptional and translational regulation.[6-8] This underscores the need for validated tools that enable the direct detection of ALS-associated proteins to determine where gene products are expressed and how they contribute to disease mechanisms.

To address this gap, we established the ALS Reproducible Antibody Platform (ALS-RAP), characterizing commercially available antibodies against 33 ALS-associated proteins using knockout cell lines as controls to generate high-quality reagents for protein expression and functional studies. With these KO-validated renewable antibodies, we systematically mapped the relative abundance of ALS-associated proteins across human induced pluripotent stem cell (iPSC)–derived and primary neurological cell types. This analysis revealed diverse and cell type–specific protein expression signatures: some proteins were broadly distributed across neurons and glia, while others were confined to specific lineages—patterns not predictable from RNA datasets alone. Strikingly, 22 proteins were expressed in glial populations, with ten dynamically regulated by inflammatory cues in microglia, the resident brain phagocytes of myeloid origin, highlighting immune-responsive pathways as an important contributor to ALS pathogenesis.

Materials and methods

Analysis of PubMed entries for each ALS-associated gene

Throughout the manuscript, we reference ALS genes using their official gene names as listed in UniProt, written in italics (e.g., *SOD1*). To refer to the corresponding proteins, we use the same gene names in regular font, as the official protein names are often too long or ambiguous for practical use.

Each target gene was queried in PubMed using two search strategies: (1) GENE_NAME[Title/Abstract] to retrieve the total number of publications associated with the gene, and (2) (GENE_NAME[Title/Abstract]) AND ("amyotrophic lateral sclerosis" [Title/Abstract]) to identify publications specifically linking the gene to ALS. Searches were performed on August 27, 2025.

Evaluation of significance of ALS-associated genes

Each candidate gene was assessed for its potential association with ALS using the evidence published at the time of this manuscript. Using the recent review of Nijs & van Damme[3] as a model, we used currently available evidence to prioritize genes for potential association with ALS in a similar manner. First, genes were qualitatively assessed for rarity of genetic variants in the general population and among individuals with ALS. Next, any reported odds ratios (OR) for risk of ALS in variant carriers were used to approximate whether genes could be considered as having "small" (OR < 1.2), "intermediate" (1.2 < OR < 10), or "high" (OR > 10) effect sizes. Genes were assigned an "uncertain" OR estimate if no OR had been published at the time of analysis. Variant frequency was assessed considering the type(s) of inheritance previously described; variants reported through GWAS or genotyping studies were designated as "common" whereas variants reported in autosomal family/pedigree-based studies were designated as "rare". If the method of discovery was poorly described or through non-genetic analyses (e.g. transcriptomic or proteomic), genes were described as having "uncertain" frequency.

RNA expression analysis

We accessed the single-cell transcriptomics resource of the Human Protein Atlas (HPA), specifically the single-nuclei brain dataset which includes single-cell RNA sequencing data generated from 2.5 million cells and mapped to 34 supercluster cell types. Data were generated from post-mortem human brain samples digested to a single cell suspension, and cell types were clustered into transcriptomic cell types.[9] Raw sequencing data was normalized using Trimmed mean of M values and expression values were presented as normalized transcripts per million (nTPM). RNA expression data for all 33 ALS genes were downloaded online from the HPA. Data were grouped together based on overall cell type (neuron, oligodendrocyte, astrocyte, microglia, etc.) and the average expression in each cell type was determined for each gene. The average neuron, oligodendrocyte, astrocyte, and microglia expression data were extracted from the overall dataset and used in downstream analyses.

In our analyses, genes were considered "expressed" if their expression values in at least three cell types were greater than the median expression value of the entire HPA dataset (9.2 nTPM). Genes were considered "barely detectable" if expression was less than the median value in at least two cell types. For a small subset of "barely detectable" genes, expression in one cell type was greater than the median value and substantially "enriched" in that cell type. We included these in the category of "expressed" genes despite the low expression in most cell types.

To describe the cell type expression patterns for each gene, we established criteria determining if mRNA expression levels for a gene is "enriched" or not in a given cell type. Cell types in which mRNA expression for a gene is "enriched" were defined as when the ratio of the expression value in that cell type to the average expression value across all cell types was greater than or equal to 1.5*. Each gene was categorized based on the "enriched" cell types. If either more than one cell type was "enriched" or no cell types were, the gene was categorized as having "low cell-type specificity".

$$*\frac{Expression\ value\ in\ given\ cell\ type}{Average\ across\ all\ cell\ types} \geq 1.5$$

String analysis

STRING analysis was performed by entering the UniProt IDs of the 33 ALS-RAP proteins into the "multiple proteins" search at string-db.org. The analysis was restricted to the "physical subnetwork", with the minimum required interaction score set to "high confidence".

Immunoblot

Cultured cells were collected in RIPA buffer supplemented with protease inhibitors. Following 30 min on ice, lysates were spun at 238,700xg for 15 min at 4°C and equal protein aliquots of the supernatants were analyzed by SDS-PAGE and immunoblot. Immunoblots were performed with large 5–16% gradient polyacrylamide gels or precast gradient gels and nitrocellulose membranes. Proteins on the blots were visualized by Ponceau staining. Blots were blocked with 5% milk, and antibodies were incubated O/N at 4°C with 5% bovine serum albumin in TBS with 0.1% Tween 20 (TBST). The peroxidase conjugated secondary antibody was incubated in a 1:10000 dilution in TBST with 5% milk for 1 hr at room temperature followed by washes. For quantitative immunoblots, nitrocellulose transfers were incubated with REVERT total protein stain to quantify the amount of protein per lane, then blocked in Odyssey Blocking buffer (TBS) and antibodies were incubated O/N at 4°C in TBS, 5% BSA and 0.2% Tween-20. The secondary antibody (Odyssey IRDye 800CW) was incubated in a 1:20000 dilution in TBST with 5% BSA for 1 hr at room temperature followed by washes. Detection of immuno-reactive bands was performed by image scan using a LI-COR Odyssey Imaging System (LI-COR Biosciences) and data analysis was done using LI-COR Image Studio Lite Version 5.2

iPSC differentiation protocols

Healthy control iPSCs from the AIW002-02 background (EDDU, McGill University) were selected for the differentiation of the following neurological cell types. In all cases, iPSCs were cultured in mTeSR1 for 5-7 days prior to differentiation.

Motor neuron differentiation

Motor neurons were differentiated from iPSCs following a previously published protocol [10,11]. Basic neural medium (BNM, 1:1 mixture of DMEM/F12 and Neurobasal, 0.5X N2, 0.5X B27, 0.5X GlutaMAX, 1X antibiotic-antimycotic, and 100 μM ascorbic acid) serves as the base medium for all other formulations used in this protocol. iPSCs were seeded on matrigel coated flasks in

neural induction medium (BNM supplemented with 2 μM SB431542, 2 μM DMH1, 3 μM CHIR99021) with a full media change performed every other day. After 6 days, cells were passaged in patterning medium (BNM supplemented with 1 μM CHIR99021, 2 μM SB431542, 2 μM DMH1, 0.1 μM retinoic acid (RA) and 0.5 μM purmorphamine (PMN)) onto poly-L-ornithine- and laminin-coated flasks and cultured for a further 6 days with a full media change performed every other day. Cells were then passaged onto poly-L-ornithine- and laminin-coated flasks in expansion medium (BNM supplemented with 3 μM CHIR99021, 2 μM SB431542, 2 μM DMH1, 0.1 μM RA and 0.5 μM PMN, and 0.5 mM valproic acid (VPA)), with a full media change performed every other day for 6 days to obtain motor neural progenitor cells (M-NPCs). M-NPCs were dissociated as single cells and seeded onto poly-L-ornithine- and laminin-coated plates in final differentiation medium (BNM supplemented with 0.5 μM RA, 0.1 μM PMN, 0.1 μM Compound E (CpdE), 10 ng/mL insulin-like growth factor-1 (IGF-1), brain-derived neurotrophic factor (BDNF), and ciliary neurotrophic factor (CNTF)), with a half media change once per week for final differentiation into motor neurons (MNs). MNs were considered mature and collected for western blotting after four weeks of differentiation.

Dopaminergic neuron differentiation

Dopaminergic neurons were differentiated from iPSCs following a protocol of floor-plate induction[12,13] with additional modifications. Briefly, iPSCs were dissociated into single cells to form embryoid bodies (EBs). EBs were grown on low-attachment plates for one week in DMEM/F12 supplemented with 1X N2 and 1X B27, in the presence of 10 μM SB431542, 200 ng/mL Noggin, 200 ng/mL sonic hedgehog, 3 μM CHIR99021 and 100 ng/mL Fibroblast growth factor 8 (FGF8). On day 7, EBs were transferred, in the same media, to poly-L-ornithine- and laminin-coated plates. On day 14, rosettes were selected semi–manually and cultured as a monolayer in DMEM/F12 supplemented with 1X N2 and 1X B27 on poly-L-ornithine- and laminin-coated plates to generate DA neural progenitor cells (DA-NPCs). DA-NPCs were passaged at a ratio of 1:3 every 5-7 days. DA-NPCs were then cultured in neurobasal medium, supplemented with 1X N2 and 1X B27, in the presence of 1 μg/mL laminin, 500 μM dibutyryl-cAMP (db-cAMP), 20 ng/mL BDNF, 20 ng/mL glial-derived neurotrophic factor (GDNF), 200 μM ascorbic acid, 100 nM CpdE and 1 ng/mL transforming growth factor β3 (TGF-β3), with a

half media change twice per week for final differentiation into dopaminergic neurons. Dopaminergic neurons were considered mature and collected for western blotting after four weeks of differentiation.

Cortical neuron differentiation

Cortical neurons were differentiated from iPSCs following a published protocol.[14] Briefly, iPSCs were dissociated using gentle cell dissociation reagent and seeded in induction medium 1 (DMEM/F12 with Glutamax supplemented with 1X N2, 1X B27, 1X MEM Non Essential Amino Acids (NEAA), 1 μg/mL Laminin, 10 μM SB431542, 200 ng/mL Noggin, 0.1% bovine serum albumin (BSA)) on matrigel-coated 6-well plates with a full media change performed daily for one week. Cells were then cultured in induction medium 2 (DMEM/F12 with Glutamax supplemented with 1X N2, 1X B27, 1X NEAA, 1 μg/mL Laminin, 0.1% BSA) with a full media change performed daily, for a further five days. To generate neurospheres, cells were transferred to a suspension culture in expansion medium (DMEM/F12 with Glutamax, 1X N2, 1X B27, 1X NEAA, 1 μg/mL Laminin, 20 ng/mL epidermal growth factor (EGF), 20 ng/mL fibroblast growth factor basic (FGFb)), for two days. The resulting neurospheres were collected and replated in expansion medium as a monolayer on a matrigel-coated dish. A second identical purification was performed. The resulting cortical neural progenitor cells (C-NPCs) were further expanded in the same expansion medium on poly-L-ornithine- and laminin-coated flasks. The next day a half media change into STEMdiff™ Forebrain Neuron Differentiation Medium (STEMdiff™ Forebrain Neuron Differentiation Kit) was performed to begin differentiation to cortical neurons. C-NPCs were maintained in this media for one week with a half media change performed every other day. A half media change to STEMdiff™ Forebrain Neuron Maturation Medium (STEMdiff™ Forebrain Neuron Maturation Kit) was then performed. Cortical neurons were maintained in this media for an additional 21 days with a half media change performed every other day until mature, at which point they were collected for western blotting.

Oligodendrocyte differentiation

Oligodendrocytes were differentiated from iPSCs following a recently published protocol.[15] The base media for all other formulations in this protocol is as follows: DMEM/F12 with Glutamax supplemented with 1X N2, 1X B27, 1X NEAA, 55 μM β-mercaptoethanol, 25 μg/mL Insulin, and

2 μg/mL heparin. First, iPSCs were directed toward a neural progenitor fate in base media supplemented with 10 μM SB31542 and 2 μM DMH1, with daily media change over eight days. Followed by patterning with 100 nM RA and 1 μg/mL PMN in base media with daily media change, for four days. Cells were then transferred from monolayer to suspension culture in the same medium for an additional eight days to form neurospheres. Oligodendrocyte precursor cells (OPCs) were then generated and expanded in suspension using OPC media (base media supplemented with 10 ng/mL PDGF-AA, 10 ng/mL IGF-1, 10 ng/mL NT-3, 5 ng/mL HGF, 60 ng/mL 3, 3′, 5-Triiodo-L-thyronine (T3), 100 ng/mL biotin, and 1 μM db-cAMP) for 10 days. Following this, the cells were plated in OPC media onto poly-L-ornithine/laminin-coated vessels with half media changes performed every other day to support further differentiation toward the OPC lineage, which continues until day 75. At this stage, cells were detached and passaged using TrypLE™ Express Enzyme. In the final differentiation step, cells were exposed to ScienCell Astrocyte Medium supplemented with ScienCell Astrocyte Growth Supplements (AGS) for 10 days. AGS was then withdrawn, and final maturation completed by reintroducing IGF-1 and T3 at the previously described concentrations for a further 10 days, with half media changes performed every other day. At this point, oligodendrocytes were considered mature and collected for western blotting.

Astrocyte differentiation

Astrocytes were differentiated from iPSCs following a previously published protocol.[16] First, iPSCs were differentiated into neural progenitor cells following the steps described above for the generation of M-NPCs. M-NPCs were dissociated as single cells and plated at a low cell density (15,000 cells/cm^2). The next day, medium was replaced with Astrocyte Differentiation Medium (ScienCell Astrocyte Medium containing AGS, 1% fetal bovine serum (FBS) (ScienCell Research Laboratories), 1% penicillin streptomycin (Wisent Bioproducts)). Cells were passaged in the same media at a ratio of 1:2 once per week and were maintained under these culture conditions for 30 days, with a half media change performed every 3-4 days. FBS was then withdrawn to promote astrocyte maturation. Cells were maintained for an additional four weeks with a half media change performed twice per week prior to astrocyte collection for western blotting.

Microglia differentiation

iPSC-derived microglia were differentiated following a published protocol.[17] Briefly, iPSCs were differentiated to hematopoietic precursor cells (iHPCs) using the STEMCELL Technologies STEMdiff™ Hematopoietic Kit. iHPCs were harvested on days 10 and 12 of iHPC differentiation and seeded on matrigel-coated 6-well plates in microglia differentiation media (MDM, DMEM/F12 HEPES no phenol red supplemented with 2X Insulin-transferrin-selenite, 2X B27, 0.5X N2, 1X Glutamax, 1X NEAA, 400 μM monothioglycerol, and 5 μg/mL insulin) + three cytokine cocktail (25 ng/mL M-CSF, 100 ng/mL IL-34, and 50 ng/mL TGF-β1) for further differentiation into microglia. Cells were supplemented with MDM + three cytokine cocktail every other day, with a full media change performed on day 12, for 24 days of iMG differentiation. On day 25 a full media change to MDM + five cytokine cocktail (25 ng/mL M-CSF, 100 ng/mL IL-34, 50 ng/mL TGF-β1, 100 ng/mL CD200, and 100 ng/mL CX3CL1) was performed, followed by supplementation with MDM + five cytokine cocktail on day 27. Microglia were considered mature and utilized for downstream experiments after 28 days of microglial differentiation.

iPSC-derived microglia treatments

For western blotting experiments, microglial polarization was induced as follows. iPSC-derived microglia were left untreated to reflect M0 polarization. iPSC-derived microglia were treated for 24 hours with 20 ng/mL interferon γ (IFNγ) + 100 ng/mL lipopolysaccharide (LPS) for M1 polarization, or with 20 ng/mL IL-4 for M2 polarization. For bulk RNA sequencing experiments iPSC-derived microglia were treated with 20 ng/mL IFNγ for 24 hours.

Human primary cell isolation and culture

Peripheral blood mononuclear cell-derived macrophages were generated as previously described (Healy et al., 2017). Briefly, peripheral blood mononuclear cells were isolated from the venous blood using Ficoll-Paque density gradient centrifugation and monocytes were positively selected using $CD14^+$ immunomagnetic beads (Miltenyi Biotec). Monocytes were differentiated in RPMI-1640 supplemented with 10% fetal bovine serum (Wisent Bioproducts), 1% penicillin streptomycin (Thermo Fisher), 1% glutamine and recombinant 25 ng/mL M-CSF for 6 days. Macrophages were polarized by treating the cells further with IFNγ (48h) and 100 ng/mL LPS (last 24h) or by treating the cells with 20 ng/mL each interleukin-4 and interleukin-13 (48h).

Fetal microglia and astrocytes were isolated as previously described (Durafourt et al., 2013, Kieran et al., 2022) from second trimester fetal cerebrum tissues. Tissues were obtained from the Birth Defects Research Laboratory, University of Washington, Seattle, USA, with maternal written consent and under approval from local ethics boards. Briefly, tissues were minced with a scalpel, digested using trypsin and DNase and filtered, following which the isolated cells were grown on a poly-L-lysine coated flask in MEM with 5% fetal bovine serum (Wisent Bioproducts), 1% penicillin streptomycin (Thermo Fisher) and 1% glutamine. After 5-7 days, the floating microglia and the adherent astrocytes were harvested separately for downstream experiments.

Bulk RNA sequencing from iPSC-derived microglia

RNA extraction was performed using the Qiagen RNeasy kit (74106), quality control, library preparation and sequencing was performed by Genome Quebec, Montreal, Canada. Library preparation was carried out using an NEBNext RNA Library Prep kit (New England Biolabs) and samples were sequenced on an Illumina Novaseq 6000. Reads were aligned to the human reference genome GRCh38 using STAR aligner [18]. Count normalization and differential gene expression analysis was performed using DESeq2 [19] using three technical replicates of iPSC-derived microglia differentiated and processed in parallel. An FDR-adjusted p-value of ≤ 0.05 and log2 fold change of -/+ 0.5 were used to determine significantly differentially expressed genes (DEGs). K-means clustering was used to aggregate IFNγ DEGs, over-representation analysis (ORA) of these clusters was performed using WebGestalt [20].

Cell culture reagents

Reagent	**Supplier**	**Catalogue Number**
3, 3′, 5-Triiodo-L-thyronine (T3)	Sigma-Aldrich	T6397
7.5% Bovine Serum Albumin (BSA)	Sigma-Aldrich	A8412
β-Mercaptoethanol	Gibco	21985023
Antibiotic-Antimycotic	Gibco	15240–062
Ascorbic acid	Sigma-Aldrich	A5960

Astrocyte Growth Supplements (AGS)	ScienCell Research Laboratories	1852
Astrocyte Medium (AM)	ScienCell Research Laboratories	1801-b
B27	Gibco	17504-044
Biotin	Sigma-Aldrich	B4639
Brain-derived Neurotrophic Factor (BDNF)	Peprotech	450–02
CD-200	Bon Opus Biosciences	C311
CHIR99021	Selleckchem	S2924
Ciliary Neurotrophic Factor (CNTF)	Peprotech	450-13
Compound E (CpdE)	STEMCELL Technologies	73954
Dibutyryl-cAMP (db-cAMP)	Carbosynth	ND07996
DMEM/F12 HEPES no phenol red	Gibco	11039021
DMEM/F12 with Glutamax	Gibco	10565-018
DMH1	Selleckchem	S7146
DNase	Thermo Fisher	18047019
Epidermal growth factor (EGF)	Peprotech	AF-100-15
Fetal Bovine Serum (FBS)	Wisent Bioproducts	080-150
Fetal Bovine Serum (FBS)	ScienCell Research Laboratories	0010
Fibroblast Growth Factor 8 (FGF8)	Peprotech	100-25
Fibroblast Growth Factor Basic (FGFb)	Peprotech	100-18B
Fractalkine (CX3CL1)	Peprotech	300-31
Gentle Cell Dissociation Reagent	STEMCELL Technologies	100-1077
Glia-derived Neurotrophic Factor (GDNF)	Peprotech	450-10
GlutaMAX	Gibco	35050-061
Heparin	Sigma-Aldrich	H3149
Hepatocyte Growth Factor (HGF)	Peprotech	100-39H

Insulin	Sigma-Aldrich	I2643
Insulin-like Growth Factor 1 (IGF-1)	Peprotech	100–11
Insulin-transferrin-selenite	Gibco	41400045
Interferon γ (IFNγ)	Peprotech	300-02
Interleukin 13 (IL-13)	Peprotech	200-13
Interleukin 34 (IL-34)	Peprotech	200-34
Interleukin 4 (IL-4)	Peprotech	200-04
L-Glutamine	Gibco	25030081
Laminin	Invitrogen	23017-015
Lipopolysaccharide (LPS)	Thermo Fisher	00-4976-93
Macrophage Colony Stimulating Factor (M-CSF)	Peprotech	300-25
Matrigel hESC-qualified matrix	Corning	354277
MEM	Gibco	11095080
MEM Non-essential Amino Acids (NEAA)	Gibco	11140035
Monothioglycerol	Sigma-Aldrich	M6145
mTeSR1	STEMCELL Technologies	85850
N2	Gibco	17502-048
Neurobasal	Gibco	21103-049
Neurotrophin 3 (NT-3)	Peprotech	450-03
Noggin	Peprotech	120-10C
Penicillin Streptomycin	Wisent Bioproducts	450-200 EL
Penicillin Streptomycin	Gibco	15140122
Platelet-derived Growth Factor AA (PDGF-AA)	Peprotech	100-13A
Poly-L-lysine	Sigma-Aldrich	P8920
Poly-L-ornithine (PO)	Sigma-Aldrich	P3655
Purmorphamine (PMN)	Sigma-Aldrich	SML-0868

Retinoic Acid (RA)	Sigma-Aldrich	R2625
RPMI-1640	Gibco	11875093
SB431542	Selleckchem	S1067
Sonic Hedgehog	Peprotech	100-45
STEMdiff™ Forebrain Neuron Differentiation Kit	STEMCELL Technologies	08600
STEMdiff™ Forebrain Neuron Maturation Kit	STEMCELL Technologies	08605
STEMdiff™ Hematopoietic Kit	STEMCELL Technologies	05310
Transforming Growth Factor β1 (TGF-β1)	Peprotech	100-21
Transforming Growth Factor β3 (TGF-β3)	Peprotech	100-36E
TrypLE Express Enzyme	Gibco	12605010
Trypsin-EDTA	Gibco	25200056
Valproic Acid (VPA)	Sigma-Aldrich	P4543

Data availability

The Supplemental Figure 1 is available on Zenodo: https://doi.org/10.5281/zenodo.17116576

Results

Genetic prioritization and initial characterization of ALS-RAP targets

We selected 33 ALS-related genes that met the criterion of well-replicated genetic inheritance, including *ACSL5*, *ALS2*, *ANG*, *ANXA11*, *ATXN2*, *C9orf72*, *CAV1*, *CCNF*, *CHCHD10*, *CHMP2B*, *FIG4*, *FUS*, *HNRNPA1*, *HNRNPA2B1*, *KIF5A*, *LGALS1*, *MATR3*, *NEK1*, *OPTN*, *PFN1*, *SETX*, *SIGMAR1*, *SOD1*, *SPG11*, *SQSTM1*, *TAF15*, *TARDBP*, *TBK1*, *TIA1*, *TUBA4A*, *UBQLN2*, *VAPB*, *VCP*. Building on the 2024 classification by Nijs and Van Damme,[3] these genes were categorized into six groups based on variant frequency and estimated pathogenic impact: (1) rare variants with high effect size, (2) rare variants with intermediate effect size, (3) rare variants with small effect size, (4) rare variants with unknown effect size, (5) common variants with unknown effect size, and (6) common variants with small effect size (Table 1). To assess the degree of characterization, PubMed searches were performed for each gene using either the gene name alone or in combination with the term "ALS" (Table 1). Results, visualized as a line scan plot (Fig. 1A), revealed that *SOD1*, *TARDBP*, *C9orf72*, and *FUS* account for 10,809 publications of the 13,173 publications retrieved across all 33 genes. In contrast, the remaining 29 genes are substantially less studied in relation to ALS and collectively comprise what we refer to as the dark ALS-ome. Among them, 8 genes—*VCP*, *OPTN*, *SQSTM1*, *TBK1*, *ANG*, *TIA1*, *HNRNPA2B1* and *CAV1*—have been investigated in other biological contexts, while the remaining 21 remain uncharacterized.

STRING analysis of the 33 ALS-related proteins revealed limited evidence of direct protein–protein interactions, with the exception of clusters among autophagy regulators (TBK1, OPTN, UBQLN2, SQSTM1) and RNA-binding proteins (TIA1, ATXN2, TARDBP, FUS, MATR3, HNRNPA1, and HNRNPA2B1) (Supplementary Fig. 1). This suggests that while these gene products may converge on shared cellular mechanisms, they likely function through distinct molecular pathways, act in different cell types, or remain insufficiently characterized to fully define their roles.

To begin uncovering such potential patterns, we next investigated cell-type-specific expression of the 33 ALS-associated genes using RNA sequencing data from the Human Protein Atlas (HPA), a publicly available repository integrating multiple omics datasets to map human gene expression

across cells, tissues, and organs. A heatmap was generated to compare RNA expression levels across neurological cell populations, with the aim of distinguishing neuron-enriched genes from those expressed in glial cells (Fig. 1B). Five expression clusters were identified: astrocyte-enriched (*SQSTM1*); microglia-enriched (*ACSL5*, *ANXA11*, *C9orf72*, *FIG4*, *FUS*, *HNRNPA1*, *SETX*, and *TBK1*); neuron-enriched (*ALS2*, *CCNF*, *KIF5A*, and *TUBA4A*); oligodendrocyte-enriched (*CAV1*, *CHMP2B*, *LGALS1*); and a group with low cell-type specificity or broad expression (*ATXN2*, *CHCHD10*, *HNRNPA2B1*, *NEK1*, *OPTN*, *PFN1*, *SOD1*, *SPG11*, *TAF15*, *TARDBP*, *UBQLN2*, *VAPB*, and *VCP*). Four genes were barely detected in neurological cell types (*ANG*, *MATR3*, *SIGMAR1*, and *TIA1*). Within all 33 ALS genes, *ACSL5*, *CCNF*, *TUBA4A* and *CAV1* showed significant expression in only a single cell type. Together, these findings suggest that ALS-associated genes are not uniformly neuron-centric but instead display diverse expression signatures across neuronal and glial lineages.

Assessment of available reagents and tool generation for ALS-RAP associated proteins

To generate and validate research tools for the 33 ALS-RAP targets and to confirm the RNA expression patterns at the protein level, we leveraged the Antibody Characterization through Open Science (YCharOS) initiative to identify high-quality antibodies. YCharOS brings together leading antibody manufacturers and knockout (KO) cell line providers to systematically characterize commercial research antibodies side-by-side in western blot (WB), immunoprecipitation (IP), and immunofluorescence (IF) using standardized, industry-endorsed KO-based protocols.[21,22] The resulting KO-based characterization data are compiled into target-specific antibody characterization reports, openly available on Zenodo (https://zenodo.org/communities/ycharos), an open-access repository hosted by the European Organization for Nuclear Research (CERN), and within the ALS section of the YCharOS Gateway on *F1000Research* (https://f1000research.com/gateways/ycharos), ensuring PubMed indexing.

We first assessed the availability of renewable antibodies (monoclonal and recombinant) for all ALS-RAP targets using CiteAb.com. Nine proteins—VCP, FUS, GLE1, UBQLN2, KIF5A, MATR3, ATXN2, OPTN, and PFN1—lacked commercial renewable antibodies. To fill this gap, the Structural Genomics Consortium (SGC) generated recombinant protein antigens and used

animal-free phage-display technology to develop single-chain variable fragment (scFv) recombinant antibodies.[23] Antibody-encoding plasmids were deposited at Addgene, allowing researchers to produce these reagents independently. SGC-derived scFv antibodies were tested alongside commercial antibodies in our characterization pipeline.

In parallel, we assessed KO cell line coverage for the 33 ALS-RAP targets. Twenty KO cell lines were available from YCharOS partners in commonly used cancer-derived lines, selected based on parental expression levels above 3.0 $\log_2$(TPM+1) in the DepMap database—an expression threshold suitable for antibody characterization studies.[21] To complete coverage, 13 additional custom KO lines were generated and are available upon request, while *VCP* was targeted with siRNA as it is an essential gene. To enhance reagent traceability and reuse, we obtained Research Resource Identifiers (RRIDs) for all antibodies[24] and KO cell lines[25] from the Antibody Registry and Cellosaurus databases, which are cited in the corresponding antibody characterization reports (Table 1).

Antibody performance and coverage for ALS-RAP proteins

We characterized 296 antibodies—comprising 288 commercially available reagents and 8 custom scFv antibodies—targeting 33 ALS-associated proteins. For 26 targets, antibodies were tested across WB, IP and IF. Six proteins—ANG, CAV1, CCNF, KIF5A, SETX, SIGMAR1 and LGALS1—were tested only in WB due to specific limitations: specialized cell treatments (e.g., cell cycle arrest for CCNF), lack of manufacturer recommendations for IP or IF (SETX, SIGMAR1, CAV1, LGALS1, ANG), or undetectable expression in culture cell lines (KIF5A). The secreted protein ANG was tested in WB and IP. For each protein, a comprehensive validation report was compiled, reviewed in collaboration with YCharOS industry partners, and published on Zenodo, with some also appearing in *F1000Research* (Fig. 2A and Table 1). Interestingly, specific and renewable antibodies were identified for most targets across applications (Fig. 2A), demonstrating that high-quality reagents are already available for the majority of disease-associated proteins. Although YCharOS characterization reports do not assign performance scores, the antibodies used in this study were chosen based on these data, and their catalogue numbers are provided in the figure legends and Materials and Methods.

CiteAb.org searches revealed that among the 64 top- and second-most-cited antibodies across 32 ALS targets (data unavailable for TUBA4A), 40 were polyclonal and 24 were renewable (Fig. 2B). These 40 polyclonals account for 7,124 literature citations, compared to 1,205 for the 24 renewable antibodies (Fig. 2C). Of the 64 antibodies, 19 were tested directly, and only 53% were confirmed specific in their recommended applications; 47% failed KO validation, yet together accounted for 828 citations. Across all targets, at least one renewable KO-validated antibody was identified in WB, IP, and IF for 94%, 73%, and 64% of the ALS proteins, respectively. For targets without renewable antibody coverage, KO-validated polyclonal antibodies were available in 3% (WB), 12% (IP), and 8% (IF) of cases. Overall, 254 of 296 antibodies detected their intended target in WB, 95 of 244 successfully immunoprecipitated their target, and 121 of 288 correctly localized their target in IF. Importantly, new validated uses were identified for 10 antibodies in WB, 64 in IP, and 30 in IF. The newly developed scFv antibodies filled key gaps; for example, the scFv against PFN1 was the only antibody—among 18 tested—capable of immunoprecipitating the protein.[26] Collectively, these results demonstrate that renewable, KO-validated antibodies cover the majority of ALS-associated proteins, enabling reproducible studies of ALS biology.

Neurological expression scan of 31 ALS-RAP proteins

To investigate protein expression patterns across neurological cell types, we differentiated human iPSCs into a range of neurons and glial cells, followed by WB analysis using identified KO-validated antibodies, prioritizing renewable antibodies. We selected iPSC-derived cells since they offer reproducible and relatively homogeneous differentiated cell populations for studying neurological cell types. Specifically, we generated lysates from iPSC-derived motor neurons, dopaminergic neurons, cortical neurons, astrocytes, oligodendrocytes and microglia; all differentiated from the same healthy control iPSC line. However, differentiation protocols and donor genetic backgrounds can influence gene expression. To address this, we complemented our iPSC-based analyses with human primary cells—we isolated human fetal astrocytes, fetal microglia, and monocyte-derived macrophages (MDM). Proteins showing predominant expression in microglia and macrophages are referred to as myeloid-enriched.

In total, we profiled 31 ALS-RAP proteins, as we had to exclude CCNF, which requires cell cycle block for detection, and KIF5A, for which no high-quality antibody could be identified. Each

protein was assessed in two independent sources of the same cell types (Fig. 3 and Supplementary Figs. 2 and 3). Expression patterns, described in alphabetical order, revealed the following:

- **ACSL5** – Predominantly expressed in myeloid cells
- **ALS2** – Strong expression in all neuronal types and fetal astrocytes, with milder expression in oligodendrocytes
- **ANG –** Secreted protein, not detectable in cell lysates
- **ANXA11 –** Primarily detected in glial cells, particularly myeloid cells, with weaker expression in neurons
- **ATXN2 –** Robustly expressed across all neuronal types with additional, milder astrocytic expression
- **C9orf72 –** Enriched in myeloid cells and weakly expressed in other cell types, with barely detectable levels in astrocytes
- **CAV1 –** Most strongly expressed in astrocytes, with weaker expression in oligodendrocytes
- **CCNF**
- **CHCHD10 –** Highly expressed in iPSC-derived microglia, fetal microglia, and MDM, moderately in neurons, and absent from astrocytes
- **CHMP2B –** Broad expression across all cell types
- **FIG4 –** More abundant in myeloid cells, weaker in neurons, and lowest in astrocytes
- **FUS –** Detected across all cell types but enriched in neurons
- **HNRNPA1** – Highest expression in neurons, oligodendrocytes, and astrocytes, and lower expression in myeloid cells
- **HNRNPA2B1 –** Highest expression in neurons, oligodendrocytes, and astrocytes, and lower expression in myeloid cells
- **KIF5A**
- **LGALS1** – Largely restricted to glial cells, also detectable in cortical neurons, but barely present in motor and dopaminergic neurons
- **MATR3 –** Broadly expressed, though only mildly in myeloid cells

- **NEK1** – Detected in neurons, oligodendrocytes, and astrocytes, with minimal levels in myeloid cells
- **OPTN** – Detectable across all cell types at comparable levels
- **PFN1** – Enriched in glial cells, particularly myeloid cells, also present in cortical neurons, but absent from dopaminergic and motor neurons
- **SETX** – Detected as a smear across cell types, with lowest levels in myeloid cells
- **SIGMAR1** – Expressed in all cell types, with highest levels in cortical neurons and iPSC-derived astrocytes, and lowest in myeloid cells
- **SOD1** – Broadly detected with relatively uniform levels, except for lower abundance in myeloid cells
- **SPG11** – Most abundant in glial cells, with weaker expression in motor and dopaminergic neurons
- **SQSTM1** – Expressed across all cell types, with highest levels in myeloid cells and motor neurons
- **TAF15** – Broadly expressed but most enriched in astrocytes
- **TARDBP** – Expressed across all cell types, with highest levels in neurons and astrocytes
- **TBK1** – Broadly expressed but highest in fetal microglia and macrophages
- **TIA1** – Expressed across cell types but barely detectable in myeloid cells
- **TUBA4A** – Primarily detected in neurons, with additional expression in glial cells but minimal levels in microglia
- **UBQLN2** – Present across all cell types, with lowest expression in myeloid cells
- **VAPB** – Primarily expressed in neurons, with additional expression in all glial cells
- **VCP –** Detected at comparable levels across all cell types

Taken together, these results highlight distinct expression patterns across the ALS-RAP protein set. A subset of proteins showed preferential neuronal enrichment (ALS2, ATXN2, FUS, HNRNPA1, HNRNPA2B1, SIGMAR1, TARDBP, TUBA4A), whereas others were most abundant in glial populations, including astrocytes (ANXA11, SPG11, TAF15, CAV1) or myeloid cells (ACSL5, C9orf72, CHCHD10, FIG4, LGALS1, PFN1, SQSTM1, TBK1). Several proteins were broadly and uniformly expressed across cell types (CHMP2B, MATR3, NEK1, OPTN,

SETX, SOD1, TIA1, UBQLN2, VCP, VAPB), while others showed more idiosyncratic patterns, such as ANG (undetectable in lysates), SQSTM1 (high in myeloid cells and motor neurons), and TBK1 (peaking in fetal microglia and macrophages).

Protein-level analyses confirmed several of the transcriptomic trends observed from our analysis of HPA sequencing data, but also revealed important divergences. For example, ACSL5, C9orf72, ANXA11, FIG4, and TBK1 were enriched in myeloid cells at both RNA and protein levels, strengthening evidence for their microglial relevance. Conversely, FUS, HNRNPA1, and SETX were predicted by RNA profiling to be microglia-enriched but were instead broadly expressed or most strongly expressed in neurons at the protein level. Several broadly expressed genes at the RNA level showed cell type–specific differences in protein abundance – in particular CHCHD10, PFN1, SPG11, and SQSTM1 showed increased protein levels in myeloid populations while TARDBP and VAPB showed increased levels in neurons. In contrast, ANG, MATR3, SIGMAR1, and TIA1, which appeared nearly absent at the RNA level, were readily detectable as proteins in multiple cell types. Collectively, these comparisons underscore that RNA abundance is only ~33% predictive of protein expression,[27] highlighting the importance of direct protein-level validation. Together, the RNA–protein comparison demonstrates that ALS-associated proteins exhibit diverse and cell type–specific expression patterns, many of which are not apparent from transcriptomic data alone. In particular, the enrichment of multiple ALS proteins in microglia and other glial populations suggests that non-neuronal cell types may contribute more directly to ALS pathogenesis than previously appreciated.

Ten ALS-associated proteins are regulated upon inflammatory stimulus

Immune-related mechanisms are increasingly recognized in ALS pathology. For example, *C9orf72* KO mice show reduced viability following immune challenge.[28] Similarly, mutations in *SETX* were recently shown to activate $CD8^+$ T cells, triggering antigen-specific motor neuron death in mice.[29] These findings suggest that immune activation and antigen presentation are important contributors to ALS-related neurodegeneration.

Microglia and macrophages exhibit remarkable plasticity, adopting a wide range of dynamic functional states in response to many intrinsic and extrinsic factors: including sex, age, spatial location, and environmental cues. Although simplistic compared to the often-layered cues

determining microglial and macrophages states *in vivo*, exposure to various cytokines and/or pathogen-associated molecular patterns (PAMPs) can influence the functional state of these cells *in vitro*. Here we utilize exposure to interferon-gamma (IFNγ) alone or in combination with lipopolysaccharide (LPS),[30] cues known to promote the release of pro-inflammatory cytokines and antimicrobial mediators, to model a pro-inflammatory state. Exposure to interleukin-4 (IL-4), which supports tissue repair, angiogenesis, and the resolution of inflammation,[31,32] was used to model an anti-inflammatory state.

Given the glial expression of many ALS-associated genes, and the preferential expression of eight proteins in microglia and macrophages, we investigated whether inflammatory stimuli influence the expression of ALS-RAP targets at both the RNA and protein level. Bulk RNA sequencing was performed on unstimulated and IFNγ-stimulated iPSC-derived microglia. Transcriptome profiling confirmed robust response of the cells to IFNγ: expression of ~50% of genes detected was differentially regulated, with ~25% of genes significantly up- or down-regulated. Using k-means clustering, genes significantly differentially expressed in response to IFNγ were broadly grouped into three clusters based on their expression (normalized counts) (Fig. 4A). Gene ontology over representation analysis revealed significant enrichment for innate immune response pathways in clusters of genes that are upregulated (clusters 1 and 3) in response to IFNγ, and significant enrichment for cell cycle pathways in the downregulated cluster 2 (Fig. 4A & B). Additionally, many known IFNγ-responsive genes[30,33-37] are observed to be significantly differentially expressed in iPSC-derived microglia (Fig. 4C). Full results of the differential gene expression analysis are presented in Supplementary Table 1. Among the 33 ALS-RAP genes, two (*CAV1* and *KIF5A*) were not detected, six (*ACSL5*, *C9orf72*, *NEK1*, *OPTN*, *TBK1*, and *TUBA4A*) were significantly upregulated, while *ATXN2*, *CCNF*, and *LGALS1* were significantly downregulated upon stimulation of iPSC-derived microglia with IFNγ (Fig. 4D).

To determine whether these transcriptional changes were reflected at the protein level, we performed immunoblotting of both iPSC-derived microglia and human fetal microglia stimulated with IFNγ and LPS, or left unstimulated, in addition to iPSC-derived microglia stimulated with IL-4 (Fig. 5). A total of 23 proteins were examined, including genes with differential RNA expression and those with primary or broad myeloid expression. Proteins with minimal myeloid

expression were excluded. Upon IFNγ and LPS stimulation, we observed an average 1.5-fold increase in protein levels (in both iPSC- and fetal-derived microglia) for ACSL5, C9orf72, MATR3, OPTN, SQSTM1, TIA1, TUBA4A, UBQLN2, and VAPB. TBK1 showed an increase of 1.4-fold). Interestingly, CHCHD10 exhibited a marked 2.9-fold decrease in protein levels despite unchanged RNA levels, suggesting post-transcriptional or post-translational regulation.

Comparison of RNA and protein profiles revealed partial concordance. Five proteins—ACSL5, C9orf72, OPTN, TBK1, and TUBA4A—showed consistent upregulation at both RNA and protein levels. Conversely, the RNA-predicted decreases in LGALS1 and ATXN2 were not observed at the protein level. Additional proteins, including MATR3, SQSTM1, TIA1, UBQLN2, and VAPB, showed increased protein expression without corresponding RNA changes, highlighting the complexity of post-transcriptional regulation in microglia.

Discussion

Understanding the cell type–specific expression of disease-associated proteins is essential for uncovering pathogenic mechanisms and identifying therapeutic targets. In ALS, one assumption has been that disease genes are primarily expressed in motor neurons. While RNA sequencing has greatly advanced our ability to infer expression patterns in neurodegenerative diseases, RNA abundance does not always correlate with protein levels, and proteomic validation is required. Using KO-validated renewable antibodies, we systematically profiled the expression of 31 ALS-associated proteins across iPSC-derived and primary neural cell types and compared these patterns with RNA data from the HPA. Both RNA and protein analyses consistently revealed that ALS-associated proteins are not predominantly neuronal but are also expressed in glial populations. Fifteen proteins showed concordance between RNA and protein, including five enriched in microglia (ACSL5, ANXA11, C9orf72, FIG4, and TBK1). In contrast, 18 proteins displayed discordant or divergent RNA–protein profiles. These findings highlight the importance of direct protein-level validation to complement transcriptomic predictions and to enhance the biological relevance of ALS disease models.

One of the most striking outcomes was the identification of ten proteins whose levels change in microglia upon pro-inflammatory stimulation, reinforcing the central role of inflammatory signaling in modulating ALS proteins and supporting the growing recognition of the neuro-immune axis in disease progression. Several of these proteins converge on autophagy and proteostasis pathways. C9orf72, in complex with SMCR8 and WDR41,[38] regulates the initiation of autophagy,[39] with SMCR8 being phosphorylated directly by TBK1.[38] TBK1 also phosphorylates the autophagy receptors OPTN[40] and SQSTM1,[41] enhancing their cargo recruitment functions. UBQLN2 links the ubiquitin-proteasome system with autophagy,[42] TIA1 regulates autophagy regulator expression,[43] and VAPB at ER–mitochondria contact sites contributes to autophagosome biogenesis.[44] Together, these proteins connect vesicle trafficking, stress response, and ubiquitin signaling to selective autophagy, highlighting a shared pathogenic axis in ALS.

This study has several limitations. First, we relied on iPSC-derived neural cell types, which capture a tractable but restricted developmental and transcriptional state within specific genetic

backgrounds. Protein absence in these models should be interpreted cautiously, as expression profiles may not reflect fully mature cells *in vivo*, and differentiation protocols can vary in efficiency across laboratories. Complementary studies using KO-validated antibodies in immunohistochemistry across developmental stages and in postmortem human tissue will be essential to validate and extend our findings. Second, our RNA and protein analyses of iPSC-derived microglia used distinct polarization conditions (RNA after IFNγ alone; protein after IFNγ + LPS), limiting direct comparability, though regulation of key proteins was concordant across datasets. Third, our RNA analysis relied on arbitrary cutoff values to define enrichment. Fourth, the antibodies used did not target post-translational modifications (PTMs), though clear PTM-dependent regulation was observed (e.g., SQSTM1 upon IFNγ and LPS stimulation). Future studies using PTM-specific antibodies or IP–mass spectrometry will be needed. Finally, our assessment of top-cited antibody performance was incomplete, as many reagents outside the YCharOS network were not tested, introducing bias toward consortium partners.

Protein expression comparisons between iPSC-derived and primary cells also warrant careful interpretation. For example, ACSL5 is robustly expressed in fetal microglia but weaker in iPSC-derived microglia, whereas TARDP shows the opposite pattern. Such discrepancies likely reflect differences in developmental stage, culture conditions, and reprogramming artifacts rather than contradictions in biology.

While we identified high-quality renewable antibodies for most ALS-associated proteins, important gaps remain. For example, no suitable antibodies were found for KIF5A in this study, although newly available recombinant reagents and KO lines from YCharOS partners should allow this target to be revisited. Polyclonal antibodies are still the most commonly used reagents for the ALS-associated proteins analyzed here; however, we were able to identify renewable, KO-validated alternatives for the majority of targets.

In sum, we investigated ALS-associated proteins across cell types at the protein level. The identification of microglia-enriched and immune-regulated proteins highlights the critical contribution of glial biology to ALS and provides a resource for refining disease models. As the platform expands to cover the full spectrum of ALS-linked genes—and potentially those

implicated in FTD—integrated proteomic profiling will be essential for deepening our understanding of disease mechanisms and therapeutic opportunities.

Acknowledgements

We would like to thank Kathleen Southern for the coordination of information exchange between laboratories involved in the ALS-RAP project. We would like to thank Abcam, ABCD Antibodies, ABclonal, Aviva System Biology, Cell Signaling Technology, Developmental Studies Hybridoma Bank, GeneTex, Revvity, Institute for Protein Innovation, MilliporeSigma, Novus Biologicals, Proteintech, R&D Systems, Thermo Fisher Scientific for providing antibodies and/or KO cell lines, free of charge, for ALS-RAP related targets. We would like to acknowledge the Birth Defects Research Laboratory, University of Washington, Seattle, USA for providing fetal tissues.

Grant Information

This work was supported by a grant from the Motor Neurone Disease Association, the ALS Association and the ALS Society of Canada to develop the ALS-Reproducibility Antibody Platform. This work was also supported by the Government of Canada through Genome Canada, Genome Quebec and Ontario Genomics (OGI-210) and by grant from the Quebec Consortium for Drug Discovery (CQDM), a grant from the Ministère de l'Économie, de l'Innovation et de l'Énergie du Québec. The Structural Genomics Consortium is a registered charity (no. 1097737) that receives funds from Bayer, Boehringer Ingelheim, Bristol Myers Squibb, Genentech, Genome Canada through Ontario Genomics Institute (grant no. OGI-196), the European Union (EU) and European Federation of Pharmaceutical Industries and Associations through the Innovative Medicines Initiative 2 Joint Undertaking (EUbOPEN grant no. 875510), Janssen, Merck (also known as EMD in Canada and the USA), Pfizer and Takeda. R.A. is supported by a Mitacs postdoctoral fellowship. This work was supported by a CIHR project grant (PJT-195804). E.A.F. is supported by a Canada Research Chair (Tier 1) in Parkinson's disease. J.P.R. is supported by an ALS Scholars in Therapeutics postdoctoral fellowship from the Sean M. Healey & AMG Center for ALS at Massachusetts General Hospital (MGH), ALS FindingACure, and FightMND. J.P.R. is supported by an ALS Scholars in Therapeutics postdoctoral fellowship from the Sean M. Healey & AMG Center for ALS at Massachusetts General Hospital (MGH), ALS FindingACure, and FightMND.

Competing Interests

The authors report no competing interests.

References

1. Rosen DR, Siddique T, Patterson D, et al. Mutations in Cu/Zn superoxide dismutase gene are associated with familial amyotrophic lateral sclerosis. *Nature*. Mar 4 1993;362(6415):59-62. doi:10.1038/362059a0

2. Goutman SA, Hardiman O, Al-Chalabi A, et al. Emerging insights into the complex genetics and pathophysiology of amyotrophic lateral sclerosis. *Lancet Neurol*. May 2022;21(5):465-479. doi:10.1016/S1474-4422(21)00414-2

3. Nijs M, Van Damme P. The genetics of amyotrophic lateral sclerosis. *Curr Opin Neurol*. Oct 1 2024;37(5):560-569. doi:10.1097/WCO.0000000000001294

4. Beland LC, Markovinovic A, Jakovac H, et al. Immunity in amyotrophic lateral sclerosis: blurred lines between excessive inflammation and inefficient immune responses. *Brain Commun*. 2020;2(2):fcaa124. doi:10.1093/braincomms/fcaa124

5. McKeever PM, Sababi AM, Sharma R, et al. Single-nucleus transcriptome atlas of orbitofrontal cortex in amyotrophic lateral sclerosis with a deep learning-based decoding of alternative polyadenylation mechanisms. *bioRxiv*. Dec 16 2024;doi:10.1101/2023.12.22.573083

6. Upadhya SR, Ryan CJ. Experimental reproducibility limits the correlation between mRNA and protein abundances in tumor proteomic profiles. *Cell Rep Methods*. Sep 19 2022;2(9):100288. doi:10.1016/j.crmeth.2022.100288

7. Tasaki S, Xu J, Avey DR, et al. Inferring protein expression changes from mRNA in Alzheimer's dementia using deep neural networks. *Nat Commun*. Feb 3 2022;13(1):655. doi:10.1038/s41467-022-28280-1

8. Liu Y, Beyer A, Aebersold R. On the Dependency of Cellular Protein Levels on mRNA Abundance. *Cell*. Apr 21 2016;165(3):535-50. doi:10.1016/j.cell.2016.03.014

9. Siletti K, Hodge R, Mossi Albiach A, et al. Transcriptomic diversity of cell types across the adult human brain. *Science*. Oct 13 2023;382(6667):eadd7046. doi:10.1126/science.add7046

10. Deneault E, Chaineau M, Nicouleau M, et al. A streamlined CRISPR workflow to introduce mutations and generate isogenic iPSCs for modeling amyotrophic lateral sclerosis. *Methods*. Jul 2022;203:297-310. doi:10.1016/j.ymeth.2021.09.002

11. Lepine S, Nauleau-Javaudin A, Deneault E, et al. Homozygous ALS-linked mutations in TARDBP/TDP-43 lead to hypoactivity and synaptic abnormalities in human iPSC-derived motor neurons. *iScience*. Mar 15 2024;27(3):109166. doi:10.1016/j.isci.2024.109166

12. Kriks S, Shim JW, Piao J, et al. Dopamine neurons derived from human ES cells efficiently engraft in animal models of Parkinson's disease. *Nature*. Nov 6 2011;480(7378):547-51. doi:10.1038/nature10648

13. C XQC, Deneault E, Abdian N, et al. Generation of patient-derived pluripotent stem cell-lines and CRISPR modified isogenic controls with mutations in the Parkinson's associated GBA gene. *Stem Cell Res*. Oct 2022;64:102919. doi:10.1016/j.scr.2022.102919

14. Maussion G, Rocha C, Abdian N, et al. Transcriptional Dysregulation and Impaired Neuronal Activity in FMR1 Knock-Out and Fragile X Patients' iPSC-Derived Models. *Int J Mol Sci*. Oct 5 2023;24(19)doi:10.3390/ijms241914926

15. Piscopo VEC, Chapleau A, Blaszczyk GJ, et al. The use of a SOX10 reporter toward ameliorating oligodendrocyte lineage differentiation from human induced pluripotent stem cells. *Glia*. Jun 2024;72(6):1165-1182. doi:10.1002/glia.24524

16. Soubannier V, Chaineau M, Gursu L, et al. Rapid Generation of Ventral Spinal Cord-like Astrocytes from Human iPSCs for Modeling Non-Cell Autonomous Mechanisms of Lower Motor Neuron Disease. *Cells*. Jan 24 2022;11(3)doi:10.3390/cells11030399

17. McQuade A, Coburn M, Tu CH, Hasselmann J, Davtyan H, Blurton-Jones M. Development and validation of a simplified method to generate human microglia from pluripotent stem cells. *Mol Neurodegener*. Dec 22 2018;13(1):67. doi:10.1186/s13024-018-0297-x

18. Dobin A, Davis CA, Schlesinger F, et al. STAR: ultrafast universal RNA-seq aligner. *Bioinformatics*. Jan 1 2013;29(1):15-21. doi:10.1093/bioinformatics/bts635

19. Love MI, Huber W, Anders S. Moderated estimation of fold change and dispersion for RNA-seq data with DESeq2. *Genome Biol*. 2014;15(12):550. doi:10.1186/s13059-014-0550-8

20. Elizarraras JM, Liao Y, Shi Z, Zhu Q, Pico AR, Zhang B. WebGestalt 2024: faster gene set analysis and new support for metabolomics and multi-omics. *Nucleic Acids Res*. Jul 5 2024;52(W1):W415-W421. doi:10.1093/nar/gkae456

21. Ayoubi R, Ryan J, Gonzalez Bolivar S, et al. A consensus platform for antibody characterization. *Nat Protoc*. Dec 17 2024;doi:10.1038/s41596-024-01095-8

22. Monteiro FL, Voskuil JLA, Williams C. YCharOS protocol for antibody validation. *Nat Protoc*. Jun 2025;20(6):1389-1390. doi:10.1038/s41596-024-01108-6

23. Hornsby M, Paduch M, Miersch S, et al. A High Through-put Platform for Recombinant Antibodies to Folded Proteins. *Mol Cell Proteomics*. Oct 2015;14(10):2833-47. doi:10.1074/mcp.O115.052209

24. Bandrowski A, Pairish M, Eckmann P, Grethe J, Martone ME. The Antibody Registry: ten years of registering antibodies. *Nucleic Acids Res*. Jan 6 2023;51(D1):D358-D367. doi:10.1093/nar/gkac927

25. Bairoch A. The Cellosaurus, a Cell-Line Knowledge Resource. *J Biomol Tech*. Jul 2018;29(2):25-38. doi:10.7171/jbt.18-2902-002

26. Ayoubi R, McDowell I, Fotouhi M, et al. The identification of high-performing antibodies for Profilin-1 for use in Western blot, immunoprecipitation and immunofluorescence. *F1000Res*. 2023;12:348. doi:10.12688/f1000research.132249.1

27. Gry M, Rimini R, Stromberg S, et al. Correlations between RNA and protein expression profiles in 23 human cell lines. *BMC Genomics*. Aug 7 2009;10:365. doi:10.1186/1471-2164-10-365

28. Burberry A, Wells MF, Limone F, et al. C9orf72 suppresses systemic and neural inflammation induced by gut bacteria. *Nature*. Jun 2020;582(7810):89-94. doi:10.1038/s41586-020-2288-7

29. Campisi L, Chizari S, Ho JSY, et al. Clonally expanded CD8 T cells characterize amyotrophic lateral sclerosis-4. *Nature*. Jun 2022;606(7916):945-952. doi:10.1038/s41586-022-04844-5

30. Kann O, Almouhanna F, Chausse B. Interferon gamma: a master cytokine in microglia-mediated neural network dysfunction and neurodegeneration. *Trends Neurosci*. Dec 2022;45(12):913-927. doi:10.1016/j.tins.2022.10.007

31. Quarta A, Berneman Z, Ponsaerts P. Neuroprotective modulation of microglia effector functions following priming with interleukin 4 and 13: current limitations in understanding their mode-of-action. *Brain Behav Immun*. Aug 2020;88:856-866. doi:10.1016/j.bbi.2020.03.023

32. Lambert C, Desbarats J, Arbour N, et al. Dendritic cell differentiation signals induce anti-inflammatory properties in human adult microglia. *J Immunol*. Dec 15 2008;181(12):8288-97. doi:10.4049/jimmunol.181.12.8288

33. Der SD, Zhou A, Williams BR, Silverman RH. Identification of genes differentially regulated by interferon alpha, beta, or gamma using oligonucleotide arrays. *Proc Natl Acad Sci U S A*. Dec 22 1998;95(26):15623-8. doi:10.1073/pnas.95.26.15623

34. Panagiotakopoulou V, Ivanyuk D, De Cicco S, et al. Interferon-gamma signaling synergizes with LRRK2 in neurons and microglia derived from human induced pluripotent stem cells. *Nat Commun*. Oct 14 2020;11(1):5163. doi:10.1038/s41467-020-18755-4

35. Hu X, Chakravarty SD, Ivashkiv LB. Regulation of interferon and Toll-like receptor signaling during macrophage activation by opposing feedforward and feedback inhibition mechanisms. *Immunol Rev*. Dec 2008;226:41-56. doi:10.1111/j.1600-065X.2008.00707.x

36. Ivashkiv LB. IFNgamma: signalling, epigenetics and roles in immunity, metabolism, disease and cancer immunotherapy. *Nat Rev Immunol*. Sep 2018;18(9):545-558. doi:10.1038/s41577-018-0029-z

37. Kang K, Bachu M, Park SH, et al. IFN-gamma selectively suppresses a subset of TLR4-activated genes and enhancers to potentiate macrophage activation. *Nat Commun*. Jul 25 2019;10(1):3320. doi:10.1038/s41467-019-11147-3

38. Sellier C, Campanari ML, Julie Corbier C, et al. Loss of C9ORF72 impairs autophagy and synergizes with polyQ Ataxin-2 to induce motor neuron dysfunction and cell death. *EMBO J*. Jun 15 2016;35(12):1276-97. doi:10.15252/embj.201593350

39. Yang M, Liang C, Swaminathan K, et al. A C9ORF72/SMCR8-containing complex regulates ULK1 and plays a dual role in autophagy. *Sci Adv*. Sep 2016;2(9):e1601167. doi:10.1126/sciadv.1601167

40. Wild P, Farhan H, McEwan DG, et al. Phosphorylation of the autophagy receptor optineurin restricts Salmonella growth. *Science*. Jul 8 2011;333(6039):228-33. doi:10.1126/science.1205405

41. Pilli M, Arko-Mensah J, Ponpuak M, et al. TBK-1 promotes autophagy-mediated antimicrobial defense by controlling autophagosome maturation. *Immunity*. Aug 24 2012;37(2):223-34. doi:10.1016/j.immuni.2012.04.015

42. N'Diaye EN, Kajihara KK, Hsieh I, Morisaki H, Debnath J, Brown EJ. PLIC proteins or ubiquilins regulate autophagy-dependent cell survival during nutrient starvation. *EMBO Rep*. Feb 2009;10(2):173-9. doi:10.1038/embor.2008.238

43. Metur SP, Song X, Mehta S, et al. Yeast TIA1 coordinates with Npl3 to promote ATG1 translation during starvation. *Cell Rep*. Jun 24 2025;44(6):115847. doi:10.1016/j.celrep.2025.115847

44. Mao D, Lin G, Tepe B, et al. VAMP associated proteins are required for autophagic and lysosomal degradation by promoting a PtdIns4P-mediated endosomal pathway. *Autophagy*. Jul 2019;15(7):1214-1233. doi:10.1080/15548627.2019.1580103

Figure legends

Figure 1: ALS-RAP targets. (A) Number of PubMed entries related to ALS-RAP genes. Black points represent the number of entries retrieved using the search term "gene name + ALS," while gray points represent entries retrieved using the gene name alone. The x-axis indicates the number of PubMed entries, and the y-axis lists the gene names. **(B)** Heatmap showing normalized RNA expression values from the Human Protein Atlas (HPA) single nuclei brain dataset.

Figure 2: Summary of antibody performance for ALS-RAP. (A) Overview of the identification of specific antibodies for ALS-RAP proteins. **(B)** Clonality of the top- and second-most-cited antibodies. **(C)** Number of citations associated with the top- and second-most-cited antibodies, grouped by antibody type. **(D)** Fraction of manufacturers' recommended antibodies that passed or failed their intended application(s). **(E)** Coverage of ALS-RAP targets across applications, grouped by antibody type. **(F)** Summary of antibodies for which we confirmed the recommended application, observed contraction (failure in claimed use), or identified new validated applications.

Figure 3: Protein expression profiling of 31 ALS-associated proteins. KO-validated antibodies targeting the indicated proteins were selected from antibody characterization reports and used for western blotting. Lysates were prepared from human iPSC-derived motor, cortical, and dopaminergic neurons, as well as iPSC-derived oligodendrocytes, astrocytes, and microglia. Primary human fetal astrocytes and microglia, along with human monocyte-derived macrophages (MDMs), were also included.

Figure 4: RNA sequencing of iPSC-derived microglia.

(A) Analysis of differentially expressed genes (DEGs) upon IFNγ treatment of iPSC-derived microglia was performed using DESeq2, an FDR-adjusted p-value of ≤ 0.05 and log2 fold change of -/+ 0.5 were used to determine significant DEGs. Z-score of DESeq2 normalized counts of all significantly regulated IFNγ DEGs across replicates of vehicle or IFNγ treated iPSC-derived microglia are shown. IFNγ DEGs were broadly grouped (cluster 1-3) based on expression patterns using k-means clustering. **(B)** Over-representation analysis reveals functional annotation of IFNγ DEG clusters. **(C)** Fold change of known IFNγ-responsive genes in IFNγ treated iPSC-derived microglia compared to vehicle treated iPSC-derived microglia. **(D)** Fold change of ALS-RAP

genes in IFNγ treated iPSC-derived microglia compared to vehicle treated iPSC-derived microglia. * $p \leq 0.05$, ** $p \leq 0.01$, *** $p \leq 0.001$, **** $p \leq 0.0001$

Figure 5: Immune regulation of ALS-RAP proteins. KO-validated antibodies targeting 23 ALS-associated proteins were selected from antibody characterization reports and used for western blotting. iPSC-derived microglia and primary fetal microglia were stimulated with IFNγ and LPS or left non-treated (NT), while iPSC-derived microglia were additionally stimulated with IL-4. Lysates from microglia were analyzed by SDS-PAGE, followed by western blotting with the indicated antibodies. Ponceau-stained membranes are shown as loading and transfer controls.

Supplementary Figure 1: STRING network analysis. Analysis of known physical interactions between ALS-related proteins.

Supplementary Figure 2: Ponceau-stained membranes corresponding to Figure 3.

Supplementary Figure 3: Repeat of protein expression profiling. As in Figure 3, specific antibodies were used for western blotting, but semi-quantitative fluorescence-based immunoblotting was employed. Lysates were prepared from different cell preparations than those used in Figure 3.

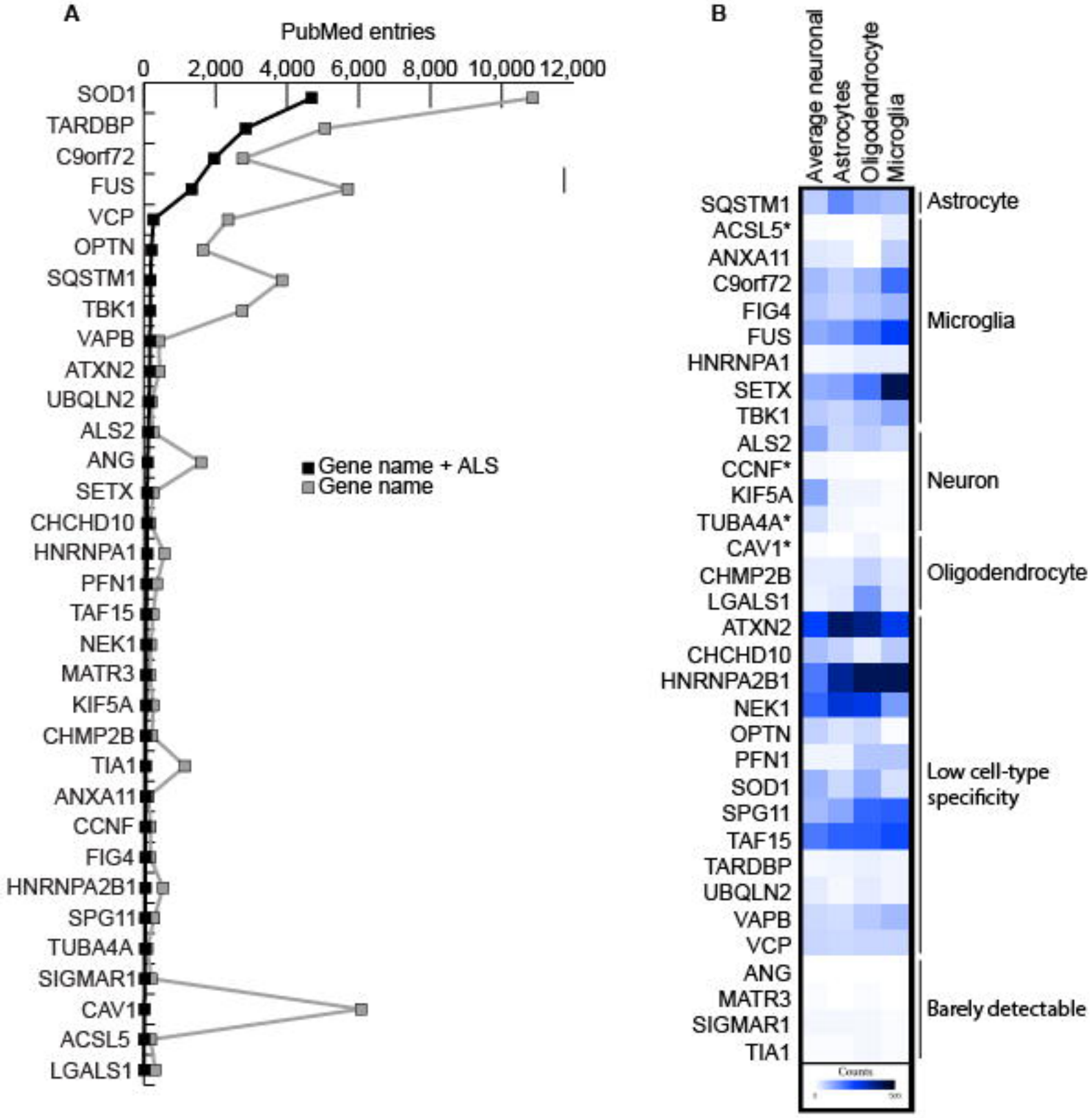

Ayoubi et al., Figure 1

A

gene name	no antibody tested	WB	IP	IF
ACSL5	8	●	■	■
ALS2	3	●	—	—
ANG	3	■	⬢	—
ANXA11	15	●	●	●
ATXN2	5	●	●	■
C9orf72	16	●	●	●
CAV1	17	●	—	—
CCNF	3	●	—	—
CHCHD10	4	●	●	●
CHMP2B	8	●	●	●
FIG4	5	●	⬢	⬢
FUS	10	●	●	●
HNRNPA1	6	●	⬢	●
HNRNPA2B1	8	●	●	●
KIF5A	4	⬢	—	—
LGALS1	11	●	—	—
MATR3	4	●	●	●
NEK1	4	■	—	—
OPTN	8	●	●	●
PFN1	16	●	●	●
SETX	11	●	—	—
SIGMAR1	5	●	⬢	⬢
SOD1	11	●	●	●
SPG11	3	●	⬢	⬢
SQSTM1	17	●	●	●
TAF15	5	●	●	●
TARDBP	18	●	●	●
TBK1	11	●	●	●
TIA1	12	●	●	●
TUBA4A	6	●	●	●
UBQLN2	10	●	●	●
VAPB	6	●	●	●
VCP	16	●	●	●

● Specific, renewable antibody identified
■ Specific, polyclonal antibody identified
⬢ No specific antibodies identified
— Application not tested

B

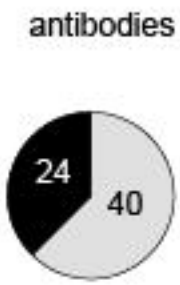

C

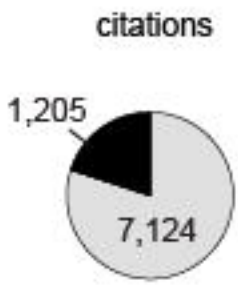

D

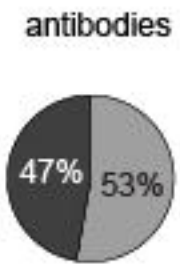

renewable antibodies
polyclonal antibodies

confirmed
failed

E

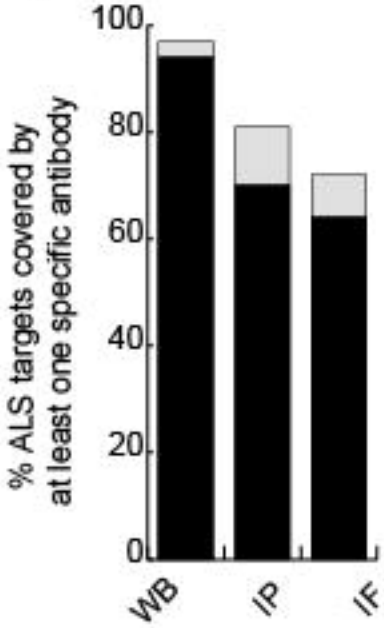

renewable antibodies
polyclonal antibodies

F

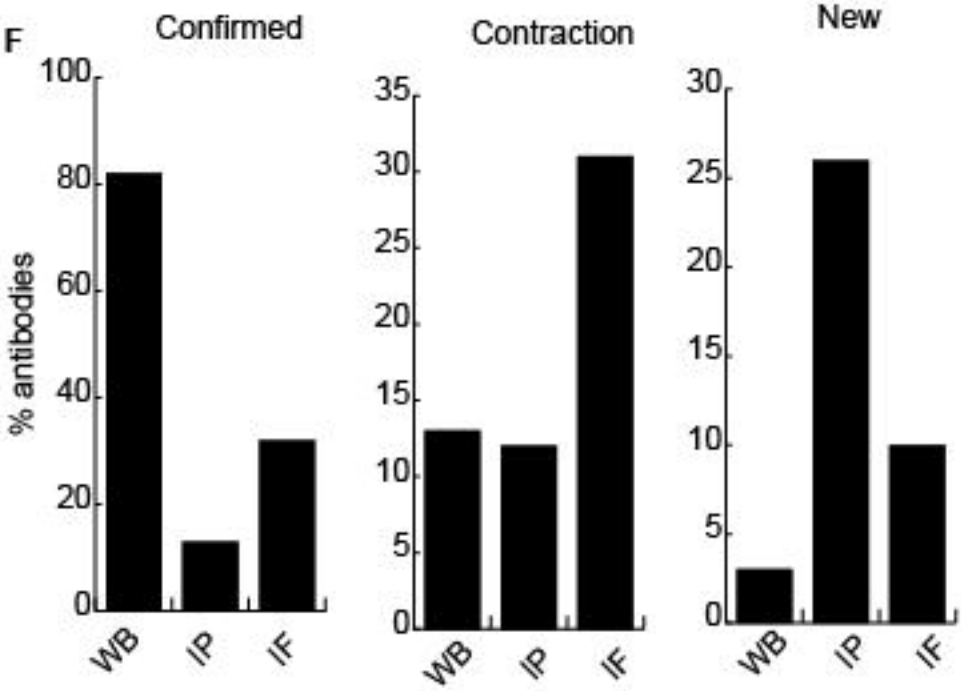

Ayoubi et al., Figure 2

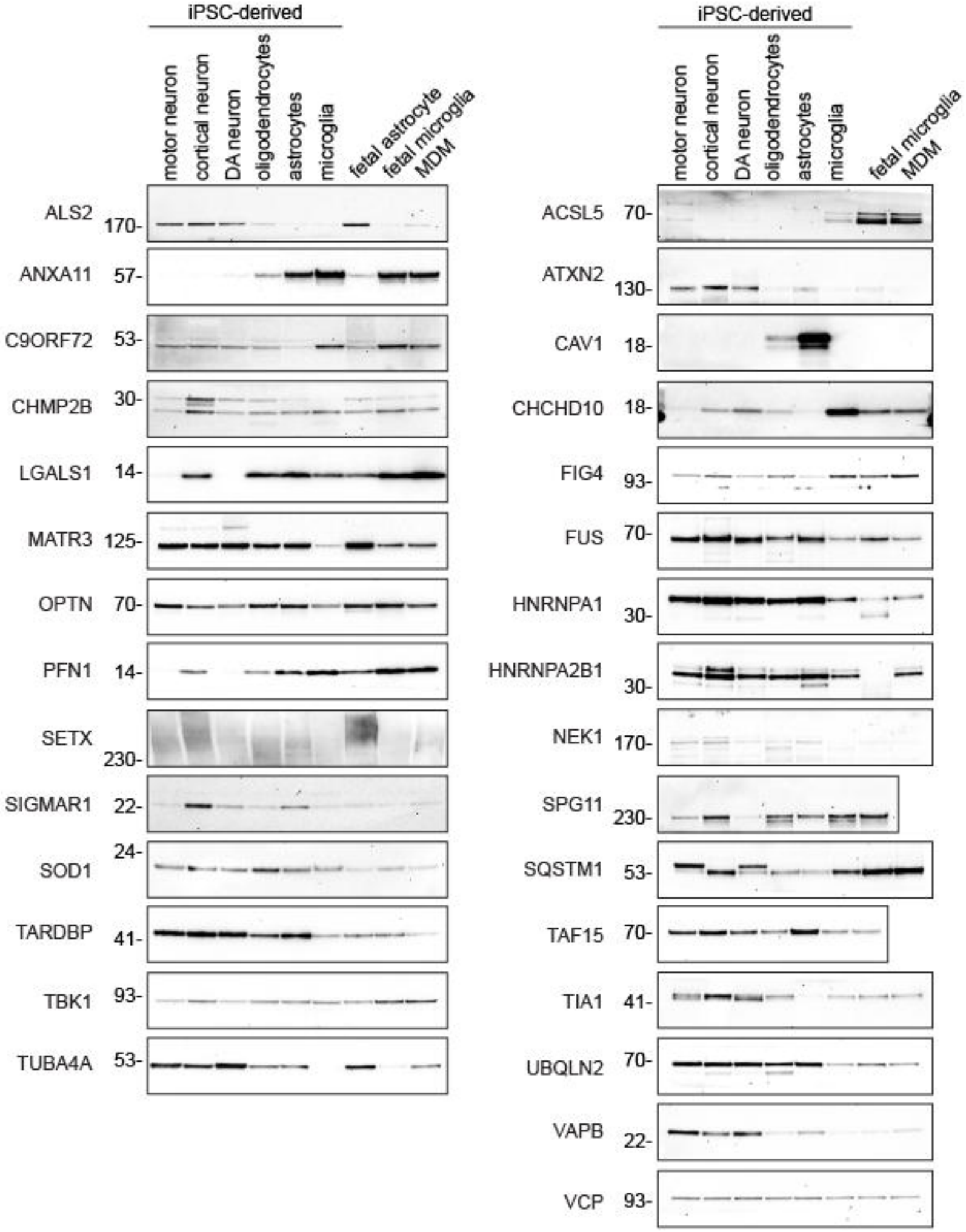

Ayoubi et al., Figure 3

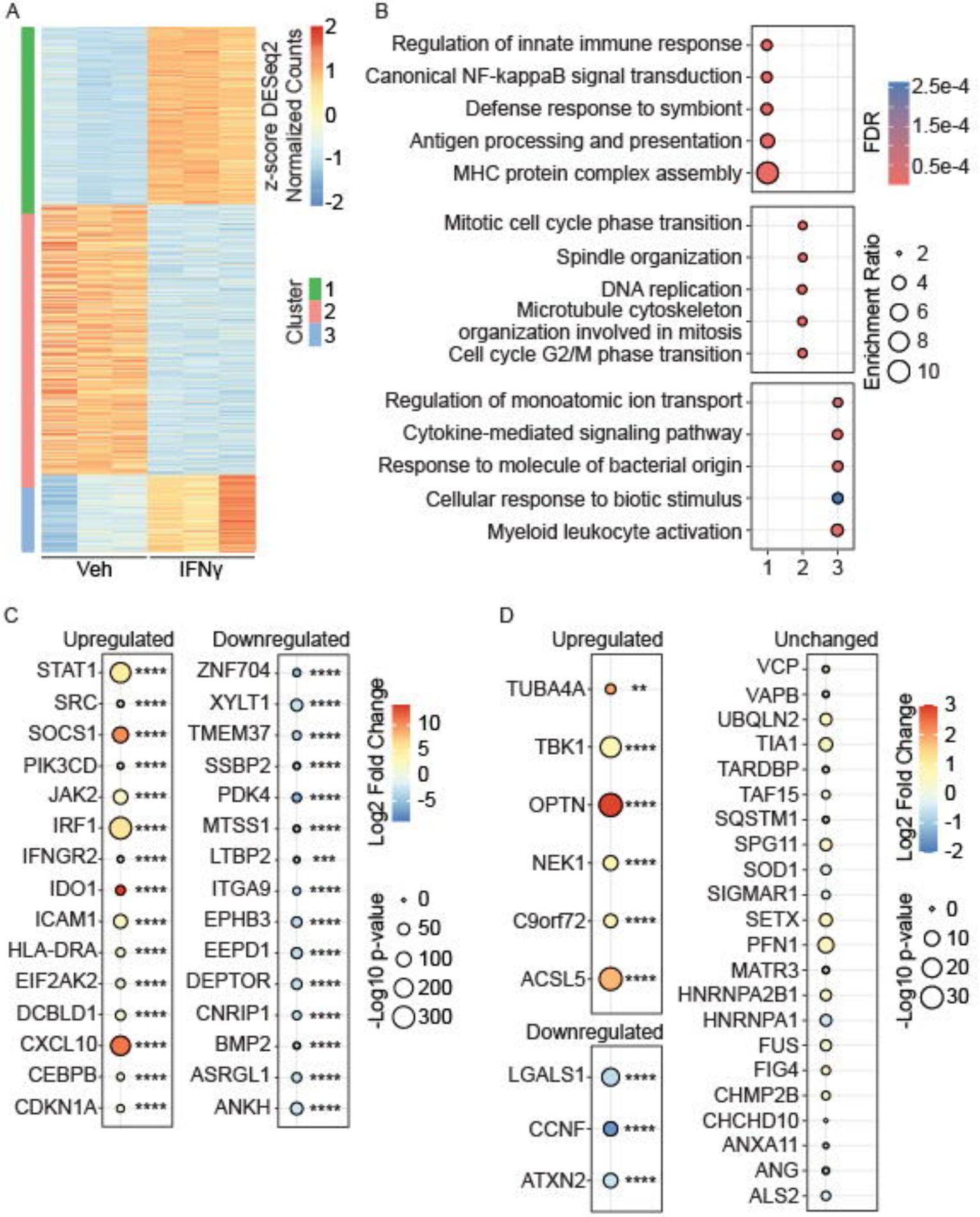

Ayoubi et al., Figure 4

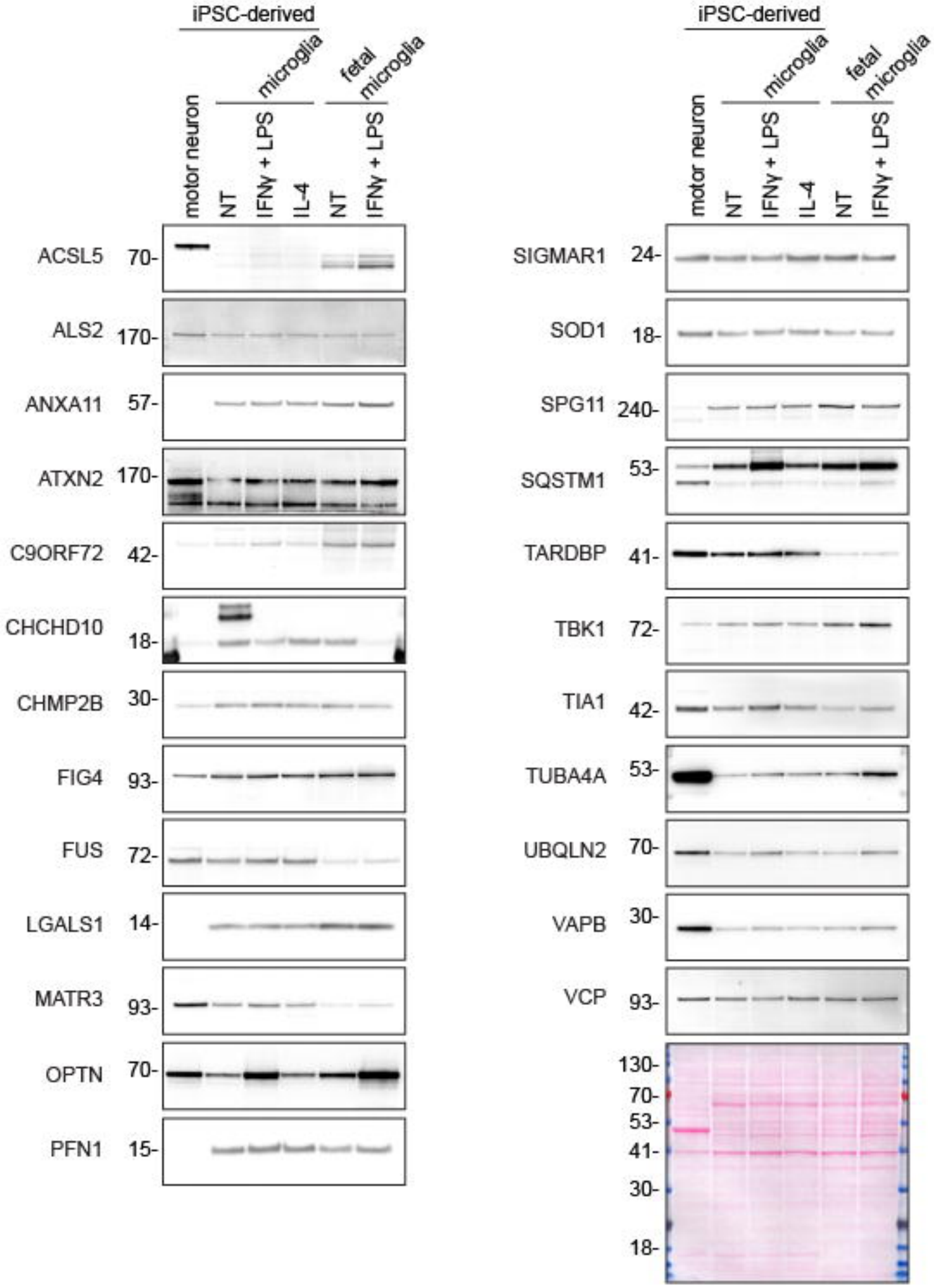

Ayoubi et al., Figure 5

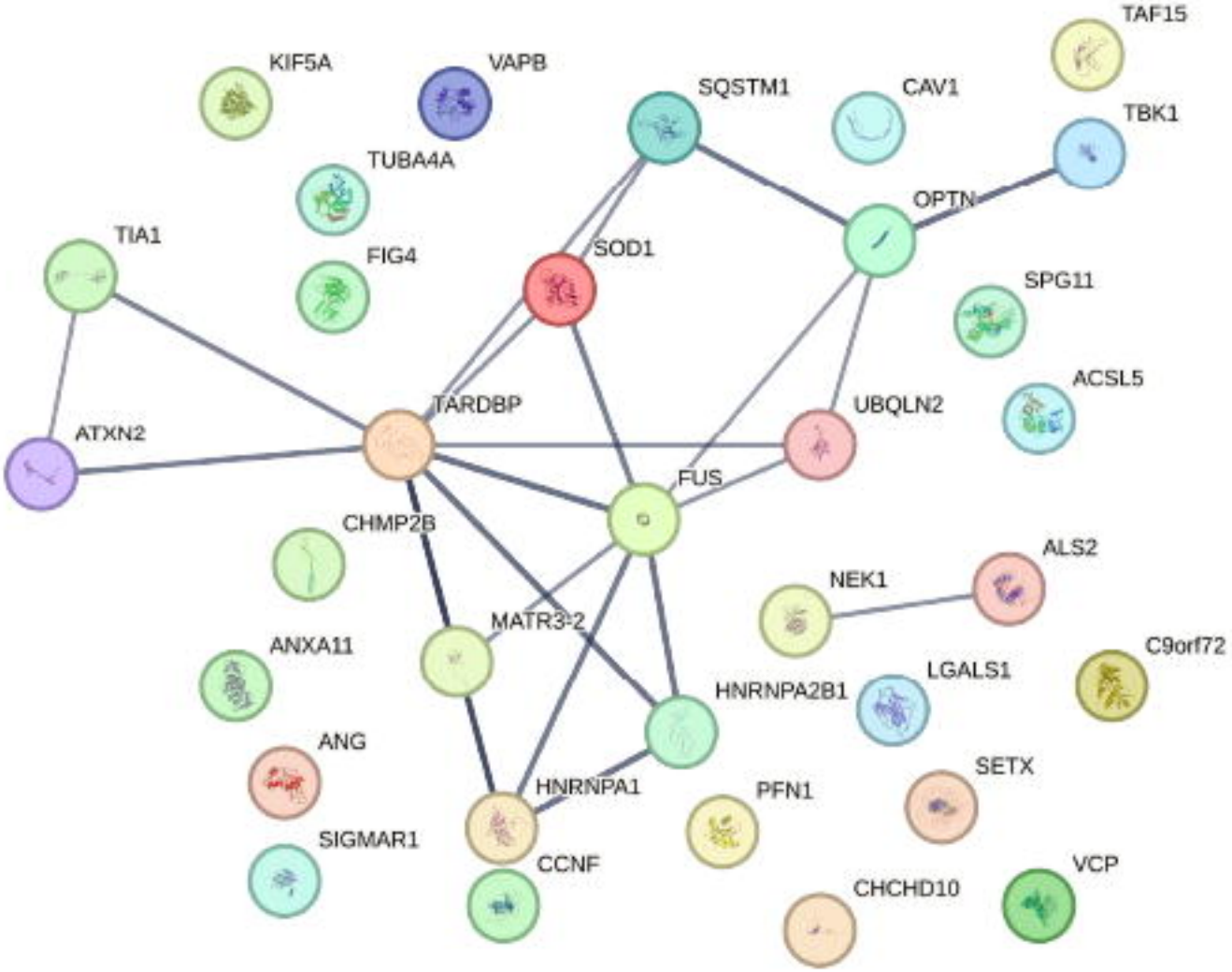

Ayoubi et al., Supplemental Figure 1

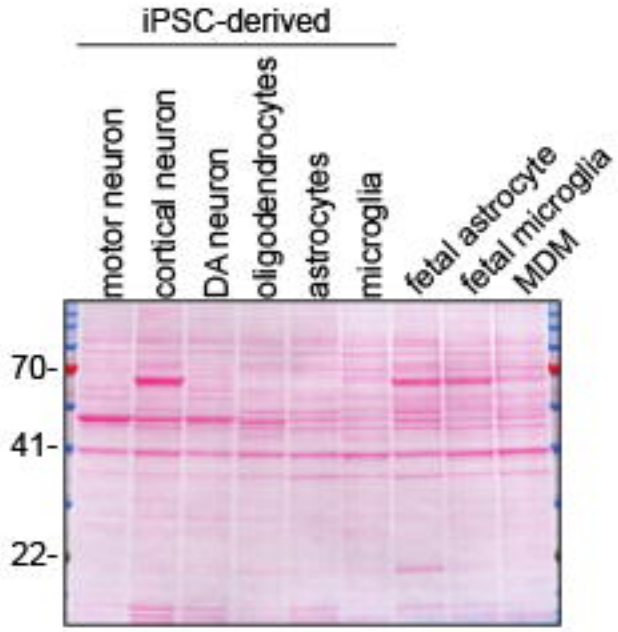

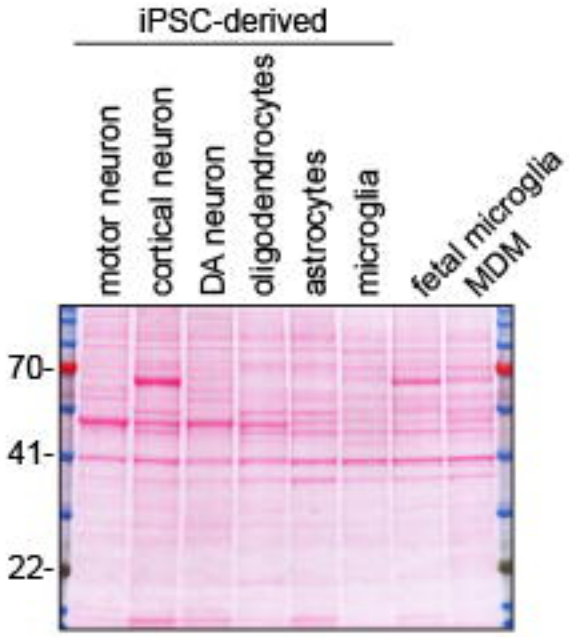

Ayoubi et al., Supplemental Figure 2

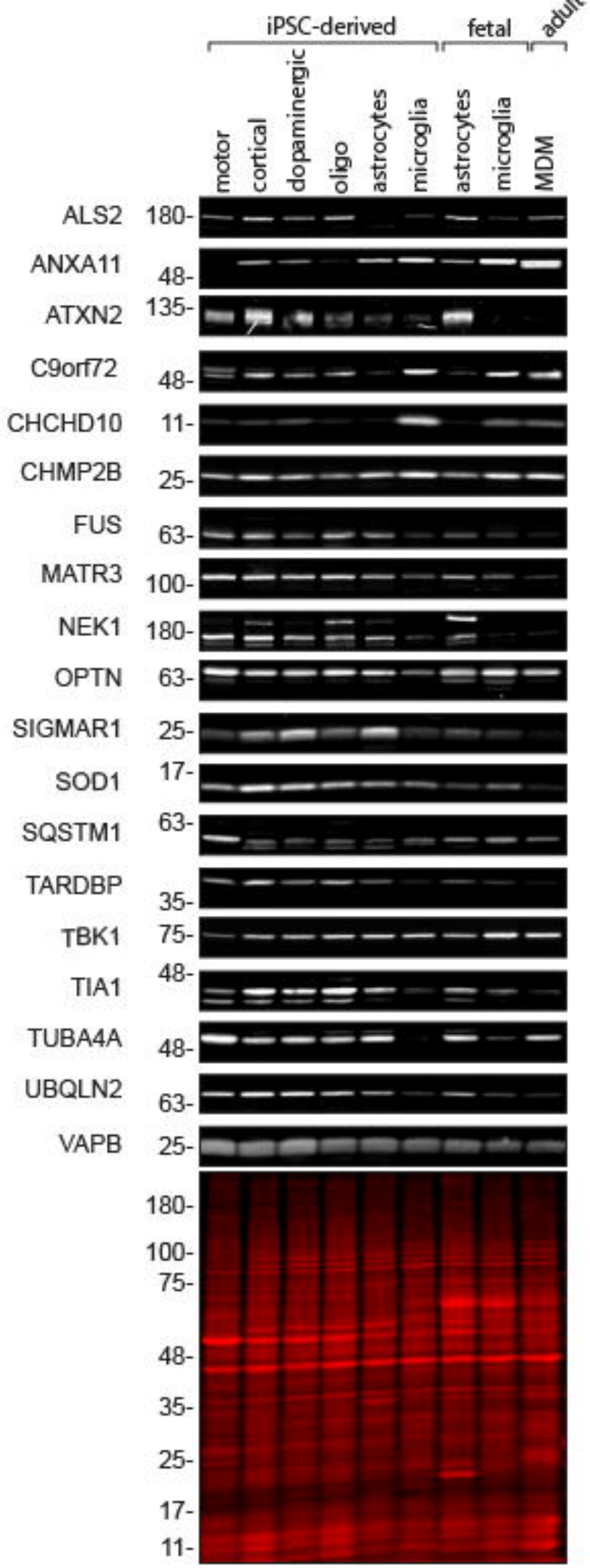

Ayoubi et al., Supplemental Figure 3

protein name	gene name	alternative protein na	Uniprot ID	Effect size	(GENE_NAM Pubmed entrie	(GENE_NAME Pubmed entries	Zenodo: YCharOS characterization reports DOI	F1000: YCharOS characterization reports DOI (if available)
Superoxide dismutase [Cu-Zn]	SOD1	Superoxide dismutase1	P00441	Rare variants with high effect size	4679	10855	https://doi.org/10.5281/zenodo.5061103	https://doi.org/10.12688/f1000research.132952.2
TAR DNA-binding protein 43	TARDBP	TDP-43*	Q13148	Rare variants with high effect size	2846	5061	https://doi.org/10.5281/zenodo.7249802	https://doi.org/10.12688/f1000research.131852.2
Guanine nucleotide exchange C9orf72	C9orf72	C9orf72	Q96LT7	Rare variants with high effect size	1952	2757	-	-
RNA-binding protein FUS	FUS	-	P35637	Rare variants with high effect size	1332	5694	https://doi.org/10.5281/zenodo.5259944	https://doi.org/10.12688/f1000research.133220.3
Transitional endoplasmic reticulum ATPase	VCP	Valosin-containing prot	P55072	Rare variants with high effect size	267	2354	https://doi.org/10.5281/zenodo.7971904	-
Optineurin	OPTN	-	Q96CV9	Rare variants with high effect size	206	1640	https://doi.org/10.5281/zenodo.10091740	-
Sequestosome-1	SQSTM1	P62	Q13501	Rare variants with intermediate effect size	183	3848	https://doi.org/10.5281/zenodo.4731001	https://doi.org/10.12688/f1000research.132628.2
Serine/threonine-protein kinase TBK1	TBK1	-	Q9UHD2	Rare variants with high effect size	178	2749	https://doi.org/10.5281/zenodo.6402968	https://doi.org/10.12688/f1000research.124632.2
Vesicle-associated membrane protein-associated protein B/C	VAPB	-	O95292	Rare variants with intermediate effect size	169	417	https://doi.org/10.5281/zenodo.13891570	https://doi.org/10.12688/f1000research.160226.1
Ataxin-2	ATXN2	SCA2	Q99700	Rare variants with intermediate effect size	163	437	https://doi.org/10.5281/zenodo.5061824	-
Ubiquilin-2	UBQLN2	-	Q9UHD9	Rare variants with high effect size	139	206	https://doi.org/10.5281/zenodo.7459541	https://doi.org/10.12688/f1000research.131851.1
Alsin	ALS2	-	Q96Q42	Rare variants with intermediate effect size	127	250	https://doi.org/10.5281/zenodo.7671674	-
Angiogenin*	ANG	-	P03950	Rare variants with intermediate effect size	99	1592	https://doi.org/10.5281/zenodo.7671286	-
Probable helicase senataxin	SETX	Senataxin	Q7Z333	Rare variants with intermediate effect size	93	257		
Coiled-coil-helix-coiled-coil-helix domain-containing protein 10, mitochondria	CHCHD10	-	Q8WYQ3	Rare variants with intermediate effect size	93	174	https://doi.org/10.5281/zenodo.5259992	https://doi.org/10.12688/f1000research.133479.2
Heterogeneous nuclear ribonucleoprotein A1	HNRNPA1	HNRPA1	P09651	Rare variants with unknown effect size	91	574	https://doi.org/10.5281/zenodo.10815038	-
Profilin-1	PFN1	-	P07737	Rare variants with intermediate effect size	79	356	https://doi.org/10.5281/zenodo.7249258	https://doi.org/10.12688/f1000research.132249.1
TATA-binding protein-associated factor 2N	TAF15	RBP56	Q92804	Rare variants with intermediate effect size	66	251	https://doi.org/10.5281/zenodo.10085319	https://doi.org/10.12688/f1000research.160371.1
Serine/threonine-protein kinase Nek1	NEK1	-	Q96PY6	Rare variants with high effect size	64	192		
Matrin-3	MATR3	-	P43243	Rare variants with unknown effect size	61	162	https://doi.org/10.5281/zenodo.10085229	-
Kinesin heavy chain isoform 5A	KIF5A	-	Q12840	Rare variants with intermediate effect size	61	259		
Charged multivesicular body protein 2b	CHMP2B	-	Q9UQN3	Rare variants with intermediate effect size	48	225	https://doi.org/10.5281/zenodo.6370501	https://doi.org/10.12688/f1000research.139755.1
Nucleolysin TIA-1 isoform p40	TIA1	-	P31483	Rare variants with intermediate effect size	47	1146	https://doi.org/10.5281/zenodo.7671718	https://doi.org/10.12688/f1000research.133645.2
Annexin A11	ANXA11	-	P50995	Rare variants with intermediate effect size	47	124	https://doi.org/10.5281/zenodo.5903684	-
Cyclin-F	CCNF	-	P41002	Rare variants with small effect size	41	184	https://doi.org/10.5281/zenodo.7971946	-
Polyphosphoinositide phosphatase	FIG4	-	Q92562	Rare variants with intermediate effect size	40	170	https://doi.org/10.5281/zenodo.10814961	-
Heterogeneous nuclear ribonucleoproteins A2/B1	HNRNPA2B1	HNRPA2B1	P22626	Rare variants with unknown effect size	38	535	https://doi.org/10.5281/zenodo.10092284	-
Spatacsin	SPG11	-	Q96JI7	Rare variants with intermediate effect size	34	283	https://doi.org/10.5281/zenodo.7459431	-
Tubulin alpha-4A chain	TUBA4A	-	P68366	Rare variants with high effect size	32	95	https://doi.org/10.5281/zenodo.7987237	-
Sigma non-opioid intracellular receptor 1	SIGMAR1	Sigma1-receptor	Q99720	Rare variants with unknown effect size	27	202	https://doi.org/10.5281/zenodo.5644356	-
Caveolin 1	CAV1	-	Q03135	Rare variants with small effect size	14	6065		
Long-chain-fatty-acid--CoA ligase 5	ACSL5	LACS 5	Q9ULC5	Common variants with small effect size	4	192	https://doi.org/10.5281/zenodo.10891256	-
Galectin-1	LGALS1	-	P09382	Rare variants with high effect size	3	308	-	-

*Instead of gene name, the corresponding term was used to search for PubMed hits